Observation of two distinct d_{xz}/d_{yz} band splittings in FeSe

P. Zhang,[1] T. Qian,[1] P. Richard,[1,2,*] X. P. Wang,[3,2,1] H. Miao,[1] B. Q. Lv,[1] B. B. Fu,[1] T. Wolf,[4] C. Meingast,[4] X. X. Wu,[1]
Z. Q. Wang,[5,1] J. P. Hu,[1,2,†] and H. Ding[1,2,‡]

[1]*Beijing National Laboratory for Condensed Matter Physics, and Institute of Physics, Chinese Academy of Sciences, Beijing 100190, China*
[2]*Collaborative Innovation Center of Quantum Matter, Beijing, China*
[3]*State Key Laboratory for Low-Dimensional Quantum Physics, Department of Physics, Tsinghua University, Beijing 100084, China*
[4]*Institut für Festkörperphysik, Karlsruhe Institute for Technology, Karlsruhe 76021, Germany*
[5]*Department of Physics, Boston College, Chestnut Hill, Massachusetts 02467, USA*

We report the temperature evolution of the detailed electronic band structure in FeSe single crystals measured by angle-resolved photoemission spectroscopy (ARPES), including the degeneracy removal of the d_{xz} and d_{yz} orbitals at the Γ/Z and M points, and the orbital-selective hybridization between the d_{xy} and $d_{xz/yz}$ orbitals. The temperature dependences of the splittings at the Γ/Z and M points are different, indicating that they are controlled by different order parameters. The splitting at the M point is closely related to the structural transition and is attributed to orbital ordering defined on Fe-Fe bonds with a d-wave form in the reciprocal space that breaks the rotational symmetry. In contrast, the band splitting at the Γ/Z points remains at temperature far above the structural transition. Although the origin of this latter splitting remains unclear, our experimental results exclude the previously proposed ferro-orbital ordering scenario.

PACS number(s): 74.70.Xa, 74.25.Jb

I. INTRODUCTION

Several experimental studies report the breakdown of the rotational symmetry in parent and underdoped compounds of Fe-based superconductors (FeSCs) [1–4] that is commonly referred to as nematicity. Its origin is highly debated since both magnetic [5–8] and orbital [9–12] fluctuations or orderings can lead to nematicity and it is often argued that nematicity might be directly related to the unconventional superconductivity in this class of materials. Although strong support is given to magnetic-driven nematicity in iron-pnictides [13] where the orthorhombic lattice distortion is always accompanied by a collinear magnetic order at a temperature equal to or below the lattice transition temperature, this mechanism is questioned in FeSe, which exhibits an orthorhombic lattice distortion below the distortion transition temperature $T_s \sim 90$ K without any trace of magnetic order. As a direct signature of the microscopic electronic anisotropy between the x and y directions in the nematic state, previous angle-resolved photoemission spectroscopy (ARPES) studies [14–16] revealed a splitting between the otherwise degenerate Fe $3d_{xz}$ and Fe $3d_{yz}$ orbitals at the M point of the Brillouin zone (BZ). This splitting is widely believed to be a key evidence for ferro-orbital ordering in the nematic phase [9,17–19].

In this paper we intend to address the symmetry of the order parameter for the orbital ordering. We report the observation of an unconventional d-wave orbital order [20,21] related to the nematicity in Fe-based superconductors. This is determined from the different splitting behaviors at the M$(\pi,0,0)$ and $\Gamma(0,0,0)$/Z$(0,0,\pi)$ points. The splitting at M is about 60 meV at 20 K and decreases with temperature increasing, and disappears at about 100–120 K, at slightly higher temperature

than T_s, due to short-range orbital order or fluctuations related to the structural transition. However, the situation is more complicated than expected as a splitting insensitive to the structural transition is also observed at the BZ center (Γ). The splitting at the Γ point is about 30 meV at 20 K and rather insensitive to temperature up to 150 K, way above T_s. Due to the strong orbital-selectivity of the hybridization between the d_{xy} orbital and the d_{xz} and d_{yz} orbitals, we conclude that the splitting at the Γ point is not simply due to spin-orbit coupling (SOC).

II. EXPERIMENT

High-quality single crystals of β-FeSe were grown by the KCl/AlCl$_3$ chemical vapor transport method. The T_c was determined to be 9 K from magnetization measurements (see Supplemental Material (SM) Part I [22]) and the structural transition is observed around 90 K [23,24]. ARPES measurements were performed at the Dreamline beamline of the Shanghai Synchrotron Radiation Facility (SSRF) using a VG-Scienta D80 electron analyzer, and at the Institute of Physics, Chinese Academy of Sciences, using a R4000 analyzer and a helium discharge lamp. The energy resolution was set to 10 meV and the angular resolution was set to $0.2°$. Clean surfaces for the ARPES measurements were obtained by cleaving the samples *in situ* in a working vacuum better than 5×10^{-11} Torr. In the text, we label the momentum values with respect to the 1 Fe/unit cell BZ.

III. RESULTS AND DISCUSSION

We show in Fig. 1 the electronic band structure of FeSe below the structural transition, as recorded with 21.212 eV photons probing the $k_z = \pi$ momentum plane. The Fermi surface (FS) [Fig. 1(a)] is formed by one hole pocket centered at Z$(0,0,\pi)$ and two electron pockets centered at A$(\pi,0,\pi)$. Based on local density approximation (LDA) calculations (SM
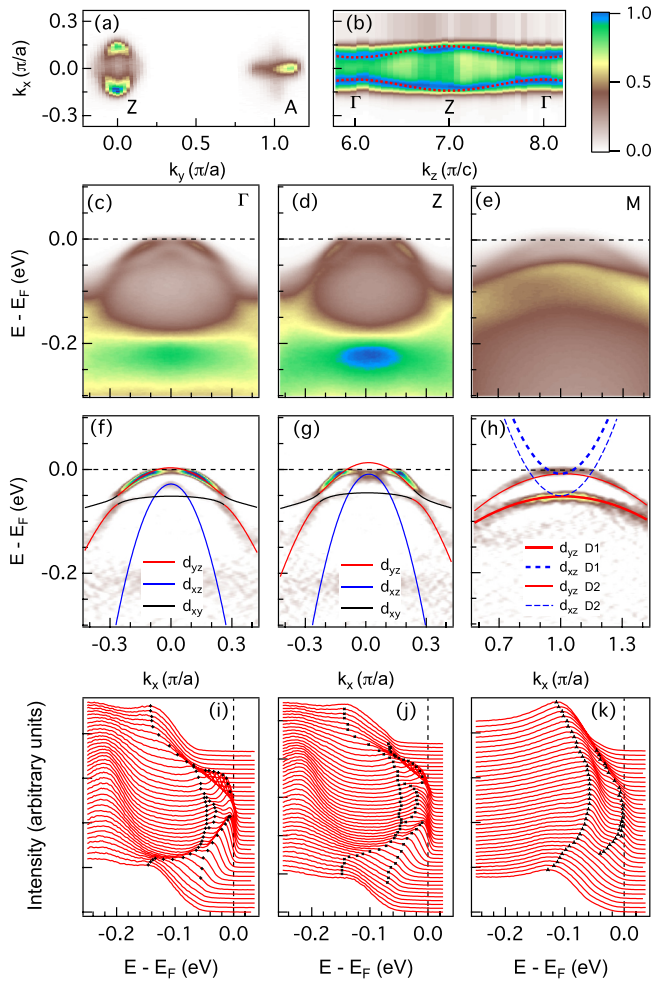
FIG. 1. (Color online) (a) FS mapping at 10 K along the Z$(0,0,\pi)$-A$(\pi,0,\pi)$ direction, recorded with unpolarized He Iα photons (21.212 eV). (b) FS mapping at 22 K along the $\Gamma(0,0,0)$-Z direction obtained in the σ geometry. The red dashed lines indicate the k_z dispersion. The intensity in (a) and (b) have been integrated in the ± 5 and ± 20 meV energy ranges, respectively. (c)–(e) Band structure at Γ, Z, and M$(\pi,0,0)$ along Γ-M or Z-A, recorded in the σ geometry, with $T = 22$ K, 22 K, and 45 K, respectively. (f)–(h) 2D curvature of (c)–(e). The red, blue, and black lines indicate the dispersions of the d_{yz}, d_{xz}, and d_{xy} orbitals, respectively. The thick and thin lines in (h) correspond to 2 different domains. (i)–(k) EDC plots of (c)–(e). The black dots indicate the EDC peaks.

Part II), we attribute the two elliptical electron pockets at A to $d_{xz/yz}$ bands in different twin domains, while the d_{xy} electron pocket is not observed. A schematic representation of the FSs ($T > T_s$) and their areas are shown in SM Part IV. As shown in Fig. 1(b), the k_z dispersion along Γ-Z is weak but non-negligible, in agreement with a previous report [25]. The Fermi wave vector (k_F) near the Γ point is $\sim 0.07\pi/a$, while it is $\sim 0.14\pi/a$ at the Z point. The small k_F can be clearly resolved from the cut at Γ displayed in Figs. 1(c), 1(f), and 1(i). Besides the d_{yz} band, we also resolve a steep d_{xz} and a flat d_{xy} bands below E_F. Interestingly, the top of the d_{xz} and d_{yz} bands do not coincide, in contrast to LDA calculations but in agreement with a previous ARPES report [16]. We also show the energy distribution curves (EDCs) and

the curvature intensity plots in Figs. 1(f)–1(h) and 1(i)–1(k), respectively. The curvature technique is based on the concept of Gaussian curvature and has been adapted recently [26] as an improvement to the second derivative method (or the Laplacian method in 2D) to facilitate the visualization of dispersive features in image plots. From the EDCs and the curvature intensity plots, we can clearly see a band splitting that we estimate to be about 30 meV at $T \sim 20$ K. As shown in Fig. 1(f), we notice that there is a large hybridization gap between the d_{yz} and d_{xy} bands near Γ but little hybridization or none between the d_{xy} and d_{xz} bands.

The band structure at Z [Figs. 1(d), 1(g), and 1(j)] is very similar, except for a relative shift along the energy direction. In particular, a splitting of about 30 meV is observed at Z between the d_{xz} and d_{yz} bands, and an hybridization gap is found between the d_{xy} and d_{yz} bands, but not between the d_{xy} and d_{xz}. In Figs. 1(e), 1(h), and 1(k), we show the band structure at M. We distinguish two hole-like bands associated with the d_{yz} bands from different twin domains. Because of a lack of coherence, the d_{xy} electron and hole bands at M are not observed. Our data indicate that the splitting at M is about 50 meV at $T \sim 50$ K, which is quite different from the prediction of onsite interactions.

To fully understand the splittings and check if they are related, we performed temperature-dependent experiments. The temperature evolution of the d_{xz}/d_{yz} splittings at high-symmetry points is illustrated in Fig. 2. Except for thermal broadening, the intensity plots show that the band dispersions around Γ barely change with temperature and that the separation between the d_{xz} and d_{yz} bands is nearly temperature independent. In other words, the d_{xz}/d_{yz} splitting at Γ is almost not changed within the temperature range studied, and the hybridization gap between the d_{xy} band and the d_{yz} band persists at high temperature, whereas no hybridization is found between the d_{xy} band and the d_{xz} band, indicating that none of these phenomena are directly related to the structural transition. Our conclusion on the splitting at Γ is reinforced by the comparison of the EDCs at the Γ point, displayed in Fig. 2(u), and at the Z point (see SM, Fig. S3).

Unlike our observation at Γ/Z, the band splitting at M varies strongly with temperature. The two sets of bands from different domains gradually merge with increasing temperature. At $T = 120$ K, we only see one set of band structure, which implies the disappearance of the domain structure, in agreement with previous results [14–16]. The evolution of the EDCs with temperature at M is shown in Fig. 2(v). The dashed lines mark the two sets of band tops/bottoms merging at $T = 120$ K.

We further fitted the EDC and momentum distribution curve (MDC) peaks together in Fig. 2(a)–2(t) with parabola to get the band dispersion, and to extract the splittings. Figure 3(a) compares the temperature dependence of the different splittings and Fig. 3(b) gives a schematic representation of the experimental splittings and hybridizations observed below and above T_s. The splittings at Γ and Z have the same amplitude, which varies very slowly with temperature, even across the structural transition. In sharp contrast, the splitting at the M point is nearly twice that at the Γ point at low temperature, but it decreases with temperature and vanishes at 100–120 K. We conclude that we must introduce two parameters to explain the data. The splitting at Γ/Z is temperature independent and
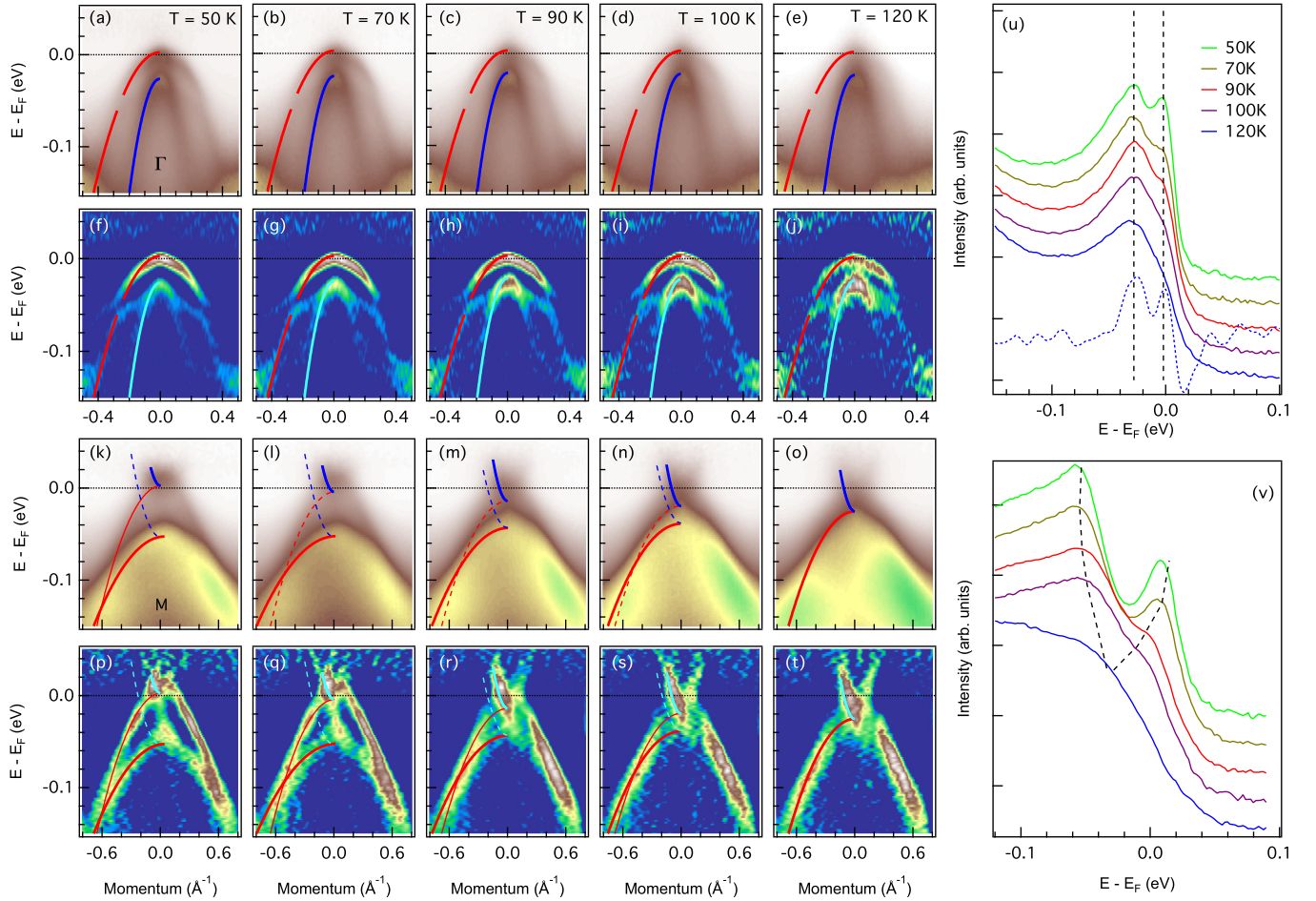
FIG. 2. (Color online) (a)–(e) ARPES intensity plots of the band structure at Γ at different temperatures. The intensity in each plot is the sum of data acquired with C^+ and C^- polarized photons. (f)–(j) EDC curvatures of (a)–(e). (k)–(o) ARPES intensity plots of the band structure at the M point at different temperatures, recorded in the σ geometry. (p)–(t) MDC curvatures of (k)–(o). (u) EDCs of (a)–(e) at $k_x = 0$. The blue dashed line is the second derivative of the blue solid line with an extra minus sign. The two dashed black lines indicate the peak positions. (v) EDCs of (k)–(o) at $k_x = 0$. The black dashed lines correspond to the EDC peaks. In all the intensity plots, the red lines represent the d_{yz} orbitals, while the blue/cyan ones represent the d_{xz} orbitals, and they are parabolic fittings of EDC and MDC peaks together. All cuts are along the Γ-M or the Z-A high-symmetry direction. All the intensities are divided by Fermi function at the corresponding temperatures.

affects only the BZ area around Γ and Z, while the parameter inducing the splitting at M only affects the M point and is related to the structural transition. Since it does not affect the splitting at the BZ center, the order parameter responsible for the splitting at the M point must have an anisotropic form of orbital order, such as the d-wave orbital order defined on the Fe-Fe bonds [20]:

$$H_{\text{bond}} = \sum_{\mathbf{k}} \frac{\Delta_{\text{M}}(T)}{4}(\cos k_x - \cos k_y)[n_{xz}(\mathbf{k}) + n_{yz}(\mathbf{k})],$$

Where $\Delta_{\text{M}}(T)$ is the temperature-dependent orbital ordering strength and $n_{xz/yz}$ are the orbital-dependent densities.

In Fig. 3(d), we provide detailed calculations and show that the d-wave orbital order can explain the experimental band structure near the M point very well with an estimated coupling constant $\Delta_0 \sim 60$ meV in the low-temperature limit.

Two major candidates for the splitting at Γ/Z are the SOC [18] and the onsite ferro-orbital fluctuations [20]. However, both explanations contain severe flaws. Indeed, SOC can break

the glide symmetry that prevents the d_{xy} band at $k + Q$ to hybridize with the d_{xz}/d_{yz} bands at k in the 1-Fe unit cell (SM Part II) [27,28]. However, such hybridization has an equal strength for both $d_{xy,\uparrow}/d_{xz,\downarrow}$ and $d_{xy,\uparrow}/d_{yz,\downarrow}$ hybridizations. Thus, the observation of hybridization between the d_{yz} and d_{xy} bands but not between the d_{yz} and d_{xy} bands is strongly against the SOC origin [29]. In addition, similar splitting at Γ has been reported to be strongly doping dependent in LiFeAs, which is apparently in contradiction with the SOC scenario [30]. The other candidate, the onsite ferro-orbital ordering or fluctuations, should remove the d_{xz}/d_{yz} degeneracy across the entire momentum space, as illustrated by our calculations shown in Fig. 3(c), which is inconsistent with the absence of splitting at M above 120 K. Together with the doping-dependent splitting observed in LiFeAs [30], we have strong reasons to believe that in FeSe the splitting at Γ and the hybridization between the d_{xy} and d_{yz} bands originate from magnetic fluctuations. The magnetism in FeSe is more frustrated than in the iron-pnictides, and long-range magnetic
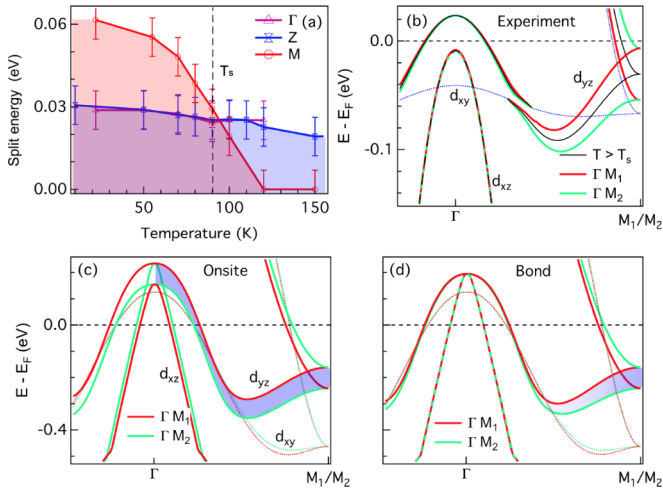
FIG. 3. (Color online) (a) Summary of the d_{xz}/d_{yz} splittings at Γ, Z, and M as a function of temperature. The splitting at M disappears at a slightly higher temperature than T_s, which might be caused by short-range ordering or fluctuations above the transition. (b) Draft of band structure extracted from experimental data and fitted with a tight binding model. The d_{xy}, d_{xz}, and d_{yz} symbols are for $T > T_s$ only since the orbital characters will change along Γ-M_1 and Γ-M_2. (c)–(d) Band structure of onsite and bond orbital order, calculated from a tight binding model (see SM Part II for the details).

ordering is thus unstable [31,32]. However, nematicity and magnetic fluctuations can still be strongly coupled [33,34].

Thus, the splitting at Γ and the hybridization between d_{xy} and d_{yz} observed above T_s are very likely signatures of this coupling. In any cases, our current results with two distinct d_{xz}/d_{yz} splittings suggest a more complicated interplay between the magnetic and orbital degrees in FeSe than previously expected.

IV. CONCLUSION

In conclusion, we report the temperature evolution of the detailed electronic band structure in FeSe single crystals. We observe two distinct d_{xz}/d_{yz} band splittings at the high-symmetry points. The splitting at M is related to the structural transition and has a d-wave form factor, while the splitting at Γ originates most likely from magnetic frustration. Our results clearly show the existence of d-wave orbital order and exclude the commonly believed ferro-orbital order, which calls for a new interpretation of the origin and implication of the orbital order in FeSCs.

[1] J.-H. Chu, J. Analytis, K. De Greve, P. McMahon, Z. Islam, Y. Yamamoto, and I. Fisher, Science **329**, 824 (2010).
[2] M. A. Tanatar, E. C. Blomberg, A. Kreyssig, M. G. Kim, N. Ni, A. Thaler, S. L. Bud'ko, P. C. Canfield, A. I. Goldman, I. I. Mazin *et al.*, Phys. Rev. B **81**, 184508 (2010).
[3] A. Dusza, A. Lucarelli, F. Pfuner, J. H. Chu, I. R. Fisher, and L. Degiorgi, Europhys. Lett. **93**, 37002 (2011).
[4] M. Yi, D. Lu, J.-H. Chu, J. G. Analytis, A. P. Sorini, A. F. Kemper, B. Moritz, S.-K. Mo, R. G. Moore, M. Hashimoto *et al.*, Proc. Natl. Acad. Sci. USA **108**, 6878 (2011).
[5] C. Fang, H. Yao, W.-F. Tsai, J.-P. Hu, and S. A. Kivelson, Phys. Rev. B **77**, 224509 (2008).
[6] Y. Qi and C. Xu, Phys. Rev. B **80**, 094402 (2009).
[7] A. Cano, M. Civelli, I. Eremin, and I. Paul, Phys. Rev. B **82**, 020408 (2010).
[8] S. Liang, A. Moreo, and E. Dagotto, Phys. Rev. Lett. **111**, 047004 (2013).
[9] C.-C. Lee, W.-G. Yin, and W. Ku, Phys. Rev. Lett. **103**, 267001 (2009).
[10] S. Onari and H. Kontani, Phys. Rev. Lett. **109**, 137001 (2012).
[11] H. Yamase and R. Zeyher, Phys. Rev. B **88**, 180502 (2013).
[12] V. Stanev and P. B. Littlewood, Phys. Rev. B **87**, 161122 (2013).
[13] R. M. Fernandes, A. V. Chubukov, and J. Schmalian, Nat. Phys. **10**, 97 (2014).
[14] K. Nakayama, Y. Miyata, G. N. Phan, T. Sato, Y. Tanabe, T. Urata, K. Tanigaki, and T. Takahashi, Phys. Rev. Lett. **113**, 237001 (2014).
[15] T. Shimojima, Y. Suzuki, T. Sonobe, A. Nakamura, M. Sakano, J. Omachi, K. Yoshioka, M. Kuwata-Gonokami, K. Ono, H. Kumigashira *et al.*, Phys. Rev. B **90**, 121111 (2014).
[16] M. D. Watson, T. K. Kim, A. A. Haghighirad, N. R. Davies, A. McCollam, A. Narayanan, S. F. Blake, Y. L. Chen, S. Ghannadzadeh, A. J. Schofield *et al.*, Phys. Rev. B **91**, 155106 (2015).
[17] Y. Zhang, C. He, Z. R. Ye, J. Jiang, F. Chen, M. Xu, Q. Q. Ge, B. P. Xie, J. Wei, M. Aeschlimann *et al.*, Phys. Rev. B **85**, 085121 (2012).
[18] R. M. Fernandes and O. Vafek, Phys. Rev. B **90**, 214514 (2014).
[19] S.-H. Baek, D. V. Efremov, J. M. Ok, J. S. Kim, J. van den Brink, and B. Büchner, Nat. Mater. **14**, 210 (2015).
[20] Y. Su, H. Liao, and T. Li, J. Phys. Condens. Matter **27**, 105702 (2015).
[21] S. Mukherjee, A. Kreisel, P. J. Hirschfeld, and B. M. Andersen, arXiv:1502.03354.
[22] See Supplemental Material at http://link.aps.org/supplemental/10.1103/PhysRevB.91.214503 for magnetization data and supplementary information on the electronic band structure.
[23] A. E. Böhmer, F. Hardy, F. Eilers, D. Ernst, P. Adelmann, P. Schweiss, T. Wolf, and C. Meingast, Phys. Rev. B **87**, 180505 (2013).
[24] A. E. Böhmer, T. Arai, F. Hardy, T. Hattori, T. Iye, T. Wolf, H. v. Loehneysen, K. Ishida, and C. Meingast, Phys. Rev. Lett. **114**, 027001 (2015).
[25] J. Maletz, V. B. Zabolotnyy, D. V. Evtushinsky, S. Thirupathaiah, A. U. B. Wolter, L. Harnagea, A. N. Yaresko, A. N. Vasiliev,

D. A. Chareev, A. E. Böhmer *et al.*, Phys. Rev. B **89**, 220506 (2014).

[26] P. Zhang, P. Richard, T. Qian, Y.-M. Xu, X. Dai, and H. Ding, Rev. Sci. Instrum. **82**, 043712 (2011).

[27] P. J. Hirschfeld, M. M. Korshunov, and I. I. Mazin, Rep. Prog. Phys. **74**, 124508 (2011).

[28] J. Hu, Phys. Rev. X **3**, 031004 (2013).

[29] We note that the broken *z*-mirror symmetry at the surface may also cause such hybridization. However, the interlayer coupling is believed to be small in FeSe, which is unlikely to cause the strong effect observed here.

[30] H. Miao, L. M. Wang, P. Richard, S. F. Wu, J. Ma, T. Qian, L. Y. Xing, X. C. Wang, C. Q. Jin, C. P. Chou *et al.*, Phys. Rev. B **89**, 220503 (2014).

[31] M. Wang, C. Fang, D.-X. Yao, G. Tan, L. W. Harriger, Y. Song, T. Netherton, C. Zhang, M. Wang, M. B. Stone *et al.*, Nat. Commun. **2**, 580 (2011).

[32] J. Hu, B. Xu, W. Liu, N.-N. Hao, and Y. Wang, Phys. Rev. B **85**, 144403 (2012).

[33] J. K. Glasbrenner, I. I. Mazin, H. O. Jeschke, P. J. Hirschfeld, and R. Valentí, arXiv:1501.04946.

[34] R. Yu and Q. Si, arXiv:1501.05926.